

# AN INVESTIGATION ON CORROSION BEHAVIOUR OF A356-10 VOL.% SiC COMPOSITES IN HCl SOLUTIONS

A. Fattah-Alhosseini<sup>1\*</sup>, M. Ranjbaran<sup>2</sup>, and S. Vajdi Vahid<sup>2</sup>

\* a.fattah@basu.ac.ir

Received: December 2014

Accepted: February 2015

<sup>1</sup> Department of Materials Engineering, Bu-Ali Sina University, Hamedan, Iran.

<sup>2</sup> Department of Materials Engineering, Faculty of Mechanical Engineering, Shahid Rajaei Teacher Training University, Tehran, Iran.

**Abstract:** In this study, corrosion behaviour of A356-10 vol.% SiC composites casted by gravity and squeeze casting is evaluated. For this purpose, prepared samples were immersed in HCl solution for 1h at open circuit potential. Tafel polarization and electrochemical impedance spectroscopy (EIS) were carried out to study the corrosion resistance of composites. The Tafel polarization and EIS studies of the corrosion behaviour of the A356-10 vol.% SiC composites showed that the corrosion resistance of the composite casted by squeeze casting was higher than that of the composites casted by gravity in selected corrosion media. Also, the Tafel polarization and EIS studies revealed that the corrosion current densities of both composites increase with the increase in the concentration of HCl. The micrographs of scanning electron microscope (SEM) clearly showed the squeeze casting composite exhibits a good dispersion/matrix interface compared to that of the composites produced by gravity casting.

**Keywords:** Composite; Corrosion; Gravity casting; Squeeze casting; Polarization.

## 1. INTRODUCTION

A356 aluminium alloy is distinguished by good mechanical characteristics, as well as excellent casting characteristics and high corrosion resistance. This alloy has been used as the basis for obtaining composites with ceramic reinforcing particles and fibers such as Al<sub>2</sub>O<sub>3</sub> and SiC [1–3]. These metal matrix composites (MMCs) have found widespread uses in many engineering applications because of their good performances, such as high strength and hardness, excellent wear resistance, low-heat expansion coefficient, competitive cost and so on [4–8].

The main disadvantage of particulate reinforced MMCs is the influence of reinforcement on the corrosion resistance. This is of particular importance in aluminium alloy based composites where corrosion resistance is imparted by a protective oxide film. The addition of a reinforcing phase could lead to further discontinuities or flaws in the protective film, increasing the sites for corrosion initiation and rendering the composite liable to severe

corrosion attack [9]. The study on the corrosion behaviour of MMCs in different aggressive environments has continued to attract considerable attention because of the several important applications of these materials. These composites frequently come in contact with acids or bases during the process like cleaning, pickling, etc. It is known that aluminium and its alloys exhibit high corrosion rate in solutions containing aggressive anions or in highly alkaline solutions [10].

Therefore, studying the corrosion behaviour of aluminium alloys and their composites in the acidic medium is of prime importance. One of the major drawbacks for gravity casting is the formation of defects such as porosity, which will be the potential crack initiators during service operation of the as cast components. The aim of this study is to compensate for the shortcomings. The squeeze casting has greater potential to create less defective cast components. Therefore, this paper deals with the corrosion behaviour of A356-10 vol.% SiC composites casted by gravity and squeeze casting in HCl solutions.

## 2. EXPERIMENTAL PROCEDURES

The chemical composition of A356 Al alloy was (wt.%): 7.5 Si, 0.33 Mg, 0.32 Zn, 0.09 Mn, 0.04 Ti, 0.16 Cu, 0.40 Fe and Al (balance). In order to prepare the composites, the alloy was first melted and raised to 700 °C in an electric furnace under controlled Argon atmosphere. The melt was maintained at this temperature for 2 min and SiC particles with 99.9% purity and 50 μm in size, were added while being stirred at 500 rpm. The schematic experimental set-up is shown in Fig. 1. To evaluate and compare the effect of casting technique on microstructure and

corrosion behavior of composites, gravity and squeeze casting were carried out separately. The parameters of the gravity and squeeze casting are shown in Table 1.

Cubic test samples were cut from cast rods and mechanically polished with abrading wet emery papers up to 2000 grit size on all sides. The samples were then embedded in cold curing epoxy resin. Prior to all measurements, working electrodes were degreased with acetone, rinsed with distilled water and dried with stream of air.

Aerated acidic solutions with three different concentrations were used. The compositions were 0.01, 0.10 and 0.50 M HCl, respectively. All

**Table 1.** The process parameters of gravity and squeeze casting.

	Gravity casting	Squeeze casting
Preheated temperature of mold (°C)	150-200	150-200
Casting temperature (°C)	700	700
Specific pressure of casting (MPa)	---	100
Velocity of filling mold (mm/s)	10	10
Pressure permanent time (s)	---	10-15
The beginning time of pressing (s)	---	5-8

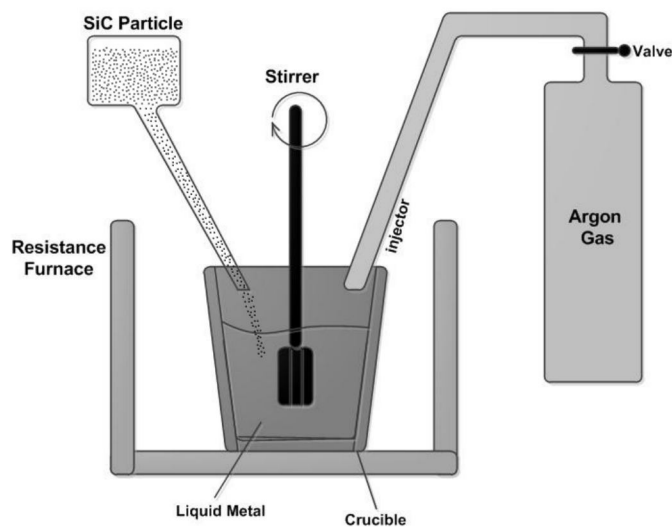


**Fig. 1.** Schematic of the experimental set-up used in the production of the composites.

solutions were made from analytical grade of 37% HCl and distilled water, and the tests were carried out at  $25 \pm 1$  °C.

All electrochemical measurements were performed in a conventional three-electrode cell under aerated conditions. The counter electrode was a Pt plate, and all potentials were measured against Ag/AgCl in saturated KCl. Electrochemical measurements were obtained using  $\mu$  autolab potentiostat/galvanostat controlled by a suitable computer. Prior to electrochemical measurements, working electrodes were immersed in open circuit potential (OCP) for 1h to form a steady-state passive film.

The Tafel curves were recorded by polarizing the specimen to -250 mV cathodically and +250 mV anodically with respect to the OCP at a scan rate of  $1 \text{ mV s}^{-1}$ . In EIS technique a small

amplitude ac signal of 10 mV peak-to-peak and frequency spectrum from 100 kHz to 10 mHz was impressed at the OCP and impedance data were analyzed using Nyquist plots. The polarization resistance was extracted from the diameter of the semicircle in the Nyquist plot. For EIS data modeling and curve-fitting method, NOVA software was used. Also, SERON-AIS-2100 SEM was used to observe the surface morphology of the composites.

### 3. RESULTS AND DISCUSSION

#### 3. 1. Microstructure

The SEM micrographs of the surfaces of the gravity and squeeze cast composites are shown in Figs. 2 and 3, respectively. As seen from Fig. 2, SEM examination of the gravity cast composite

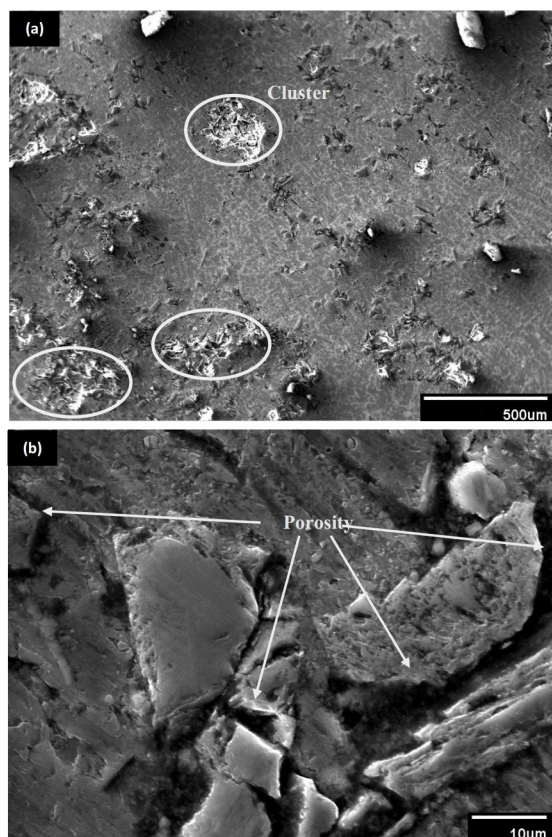


Fig. 2. SEM micrograph showing surfaces of gravity casting composite.

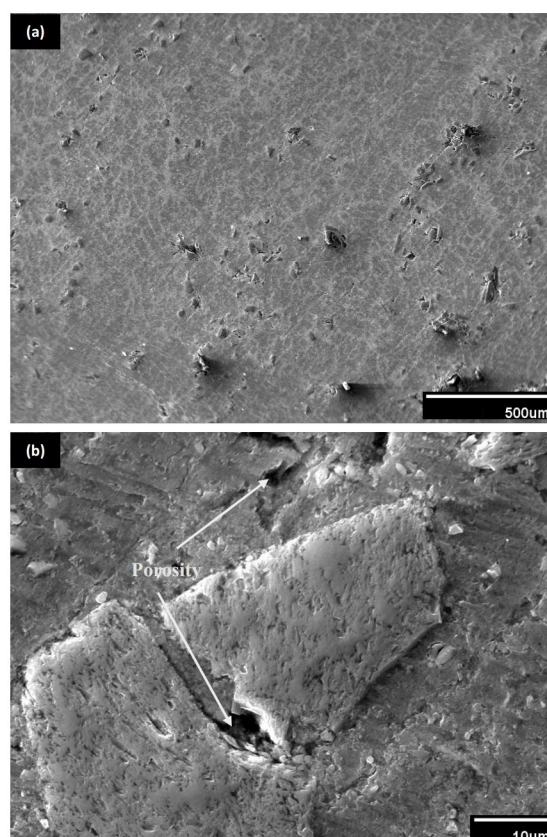


Fig. 3. SEM micrograph showing surfaces of squeeze casting composite.

demonstrated significant porosity throughout the specimen and frequent clustering of SiC particles around these pores. The porosity content of the gravity cast composite was evidently higher than that of the squeeze cast composite (Fig. 3). During solidification process the phases in composites shrink asynchronously due to the tremendous differences in heat properties. So looseness and shrinkage cavity will be brought about in the as-cast sample.

Generally, the gravity casting defects can be reduced by squeeze casting. The new casting technique means crystallizing, solidifying and plastic deforming under high pressure, which combines the compulsory feeding and compaction. Before the punch clamps down the melt has formed a chill shell. When the punch contacts the melt the whole molten composite is enclosed in the die. Then the solidifying shell will deform and feed plastically [5]. Meanwhile the melt at the front of the solidifying region will be squeezed into the gaps due to shrinkage under high pressure.

### 3. 2. Tafel Polarization Measurements

Fig. 4 illustrates the Tafel polarization curves recorded for the gravity and squeeze casting composites in HCl solutions with different concentrations. The corrosion potential and corrosion current density at different concentrations of HCl solutions for both composites are summarized in Table 2. It is seen from the data that the corrosion current density of the composite casted by squeeze casting was lower than that of the composites casted by gravity. Also, the results revealed that the corrosion current densities of both composites increased with the increase in the concentration of HCl solutions.

It is also evident from the Fig. 4 and the data in the Table 2 that the corrosion potential values are shifted in the negative potential direction with the increase in the concentration of HCl (except 0.01M). The trend is similar for both composites. The decrease in corrosion potential ( $E_{corr}$ ) value indicates loss of passivity due to thinning the primary oxide layer by chemical dissolution. Acidic corrosion of aluminium involves the

dissolution of aluminium and formation of aluminium hydroxide as partial anodic reactions together with the oxygen/water reduction and formation of hydrogen bubbles as partial cathodic reactions [11]. Therefore when aluminium is immersed in aqueous solutions, formation of the hydroxide film through incorporation and diffusion of ions into the film is occurring simultaneously with dissolution at the

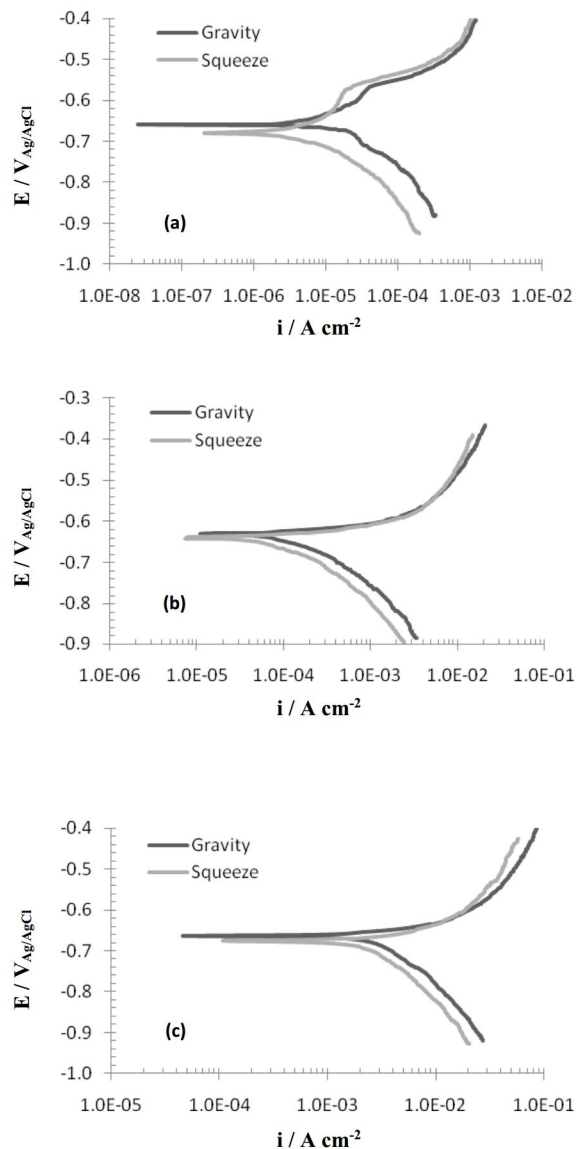


**Fig. 4.** Tafel plots of A356-10 vol.% SiC composites cast by gravity and squeeze casting in (a) 0.01M, (b) 0.10M and (c) 0.50M HCl solutions.

**Table 2.** Results of Tafel polarization studies for the corrosion behavior of A356-10 vol.% SiC composites cast by gravity and squeeze casting in HCL solutions.

HCl Solutions	Casting	$E_{corr}$ ( $V_{Ag/AgCl}$ )	$i_{corr}$ ( $A\ cm^{-2}$ )
0.01 M	Gravity	-0.659	$1.6 \times 10^{-5}$
	Squeeze	-0.679	$2.9 \times 10^{-6}$
0.10 M	Gravity	-0.631	$1.1 \times 10^{-4}$
	Squeeze	-0.648	$6.2 \times 10^{-5}$
0.50 M	Gravity	-0.663	$2.8 \times 10^{-3}$
	Squeeze	-0.676	$1.9 \times 10^{-3}$

film/solution interface, the formation and the dissolution of the film being in dynamic equilibrium. In addition, anions present in the solution can participate to the dissolution reaction through the formation of transitory complexes.

### 3. 3. EIS Measurements

Nyquist plots for the corrosion of the gravity and squeeze cast composites in 0.01M HCl solution are given in Fig.5. As can be seen from Fig.5 the impedance diagrams show semicircles, indicating that the corrosion process is mainly charge transfer controlled. The general shapes of the curves are identical for both composites in this solution, with a large capacitive loop at higher frequencies and a small inductive loop at intermediate frequencies, followed by a second capacitive loop at lower frequency values. Similar plots have been reported for the corrosion of 6061 Al-15% vol.% SiC in 1:1 mixture of hydrochloric acid and sulphuric acid medium [12].

The high frequency capacitive loop could be assigned to the charge transfer of the corrosion process and to the formation of oxide layer. The oxide film is considered to be a parallel circuit of

a resistor due to the ionic conduction in the oxide film, and a capacitor due to its dielectric properties. According to Brett the capacitive loop is corresponding to the interfacial reactions, particularly, the reaction of aluminium oxidation at the metal/oxide/electrolyte interface. The process includes the formation of  $Al^+$  ions at the metal/oxide interface, and their migration through the oxide/ solution interface where they are oxidized to  $Al^{3+}$ . At the oxide/solution interface,  $OH^-$  ions are also formed. The inductive loop at intermediate frequencies may be due to the relaxation process in the oxide layer, present on the metal surface by the adsorbed intermediate species as  $OH-Ads$ . The second capacitive loop observed at low frequencies could be assigned to the metal dissolution.

The equivalent circuit depicted in Fig. 6 [13] was used to simulate the measured impedance data on both composites in 0.01M HCl solution and provided excellent fitting. This equivalent circuit is composed of a Faradaic impedance parallel to a double layer constant phase element,  $Q_{dl}$ . Faradaic impedance consists of  $R_{ct}$  ( $= R_1 + R_2$ ) indicating the charge transfer resistance at the metal/oxide film interface,  $L$  resulting from the interruption of anodic dissolution of Al by the surface charge build-up,  $R_f$  being the resistance against charge transport in the oxide film and  $C_f$  due to the dielectric properties of surface oxide film. The  $R_s$

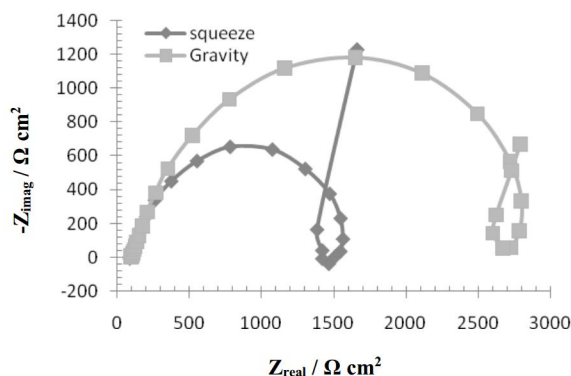


**Fig. 5.** Nyquist plots of A356-10 vol.% SiC composites cast by gravity and squeeze casting in 0.01M HCl solution.

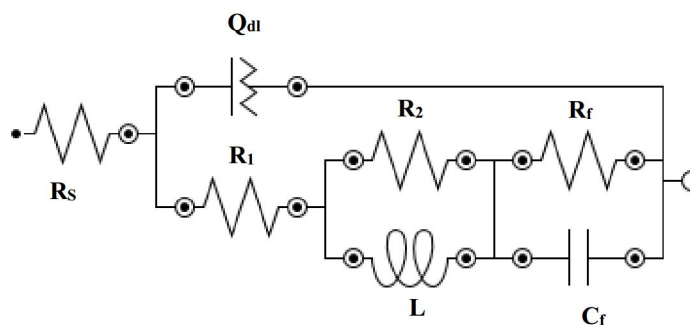


Fig. 6. The equivalent circuit used to model the Nyquist plots of both composites in 0.01M HCl solution [14].

Table 3. Best fitting parameters of the corrosion behavior of A356-10 vol.% SiC composites cast by gravity and squeeze casting in 0.01M HCl solution.

Casting	$R_s$ ( $\Omega \text{ cm}^2$ )	$R_1$ ( $\Omega \text{ cm}^2$ )	$CPE_{dl}$ ( $\mu\Omega^{-1} \text{ cm}^{-2} \text{ s}^{-n}$ )	$n_{dl}$	$R_2$ ( $\Omega \text{ cm}^2$ )	$L$ (H)	$R_f$ ( $\Omega \text{ cm}^2$ )	$C_f$ (mF)	$R_p$ ( $\Omega \text{ cm}^2$ )
Gravity	89.5	2473	56.13	0.80	776	589	3086	20.7	5559
Squeeze	88.2	1357	62.76	0.78	477	199	8556	22.6	9913

component in the circuit is a solution resistance with the value at a high frequency intercept on the real impedance axis. Table 3 presents the best fitting parameters obtained for the measured impedance data on both composites in 0.01 M HCl solution. The polarization resistance ( $R_p$ ) might be represented by the sum of  $R_1$  and  $R_f$  in the equivalent circuit.

Fig. 7 show the Nyquist plots of both composites in 0.10 and 0.50 M HCl solutions. As can be seen from Fig. 7, Nyquist plots in both solutions show a capacitive loop at high frequencies and an inductive loop at low frequencies. Similar Nyquist plots have been reported for the corrosion of 6061 Al-15% vol.% SiC in 1:1 mixture of HCl and  $H_2SO_4$  medium [12]. The high frequency capacitive loop could be assigned to the charge transfer of the corrosion process and to the formation of oxide layer and the low frequency inductive loop may be related to the relaxation process obtained by adsorption and incorporation of chloride ions on and into the oxide film. Indeed, the origin of the inductive loop can be attributed to surface or bulk relaxation of species in the oxide layer. The low

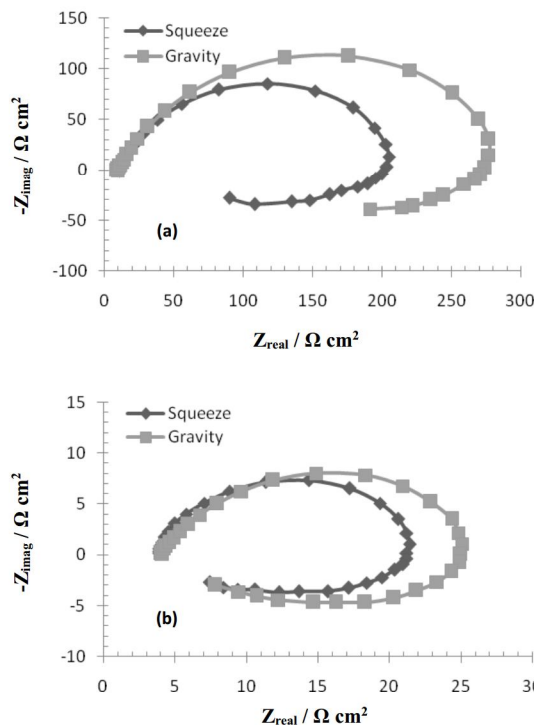


Fig. 7. Nyquist plots of A356-10 vol.% SiC composites cast by gravity and squeeze casting in (a) 0.10M and (b) 0.50M HCl solutions.

**Table 4.** Best fitting parameters of the corrosion behavior of A356-10 vol.% SiC composites cast by gravity and squeeze casting in 0.10 and 0.50M HCl solutions.

HCl Solutions	Casting	$R_s$ ( $\Omega \text{ cm}^2$ )	$CPE_{dl}$ ( $\mu\Omega^{-1} \text{ cm}^{-2} \text{ s}^{-n}$ )	$n_{dl}$	$R_{ct}$ ( $\Omega \text{ cm}^2$ )	$R_L$ ( $\Omega \text{ cm}^2$ )	L (H)	$R_p$ ( $\Omega \text{ cm}^2$ )
0.10 M	Gravity	8.24	151	0.80	275	112	4301	79
	Squeeze	8.04	118	0.81	194	168	1304	89
0.50 M	Gravity	4.10	318	0.82	19.7	6.5	46.2	4.9
	Squeeze	4.05	457	0.73	18.6	9.4	43.6	6.1

frequency inductive loop may be related to the relaxation process obtained by adsorption and incorporation of oxide ion and charged intermediates on and into the oxide film [14].

The equivalent circuit depicted in Fig.8 [15] was used to simulate the measured impedance data on both composites in 0.10 and 0.50 M HCl solutions and provided excellent fitting. This equivalent circuit consists of a constant phase element ( $Q_{dl}$ ) in parallel with the parallel resistors  $R_{ct}$  (charge transfer resistance) and  $R_L$  (inductance resistance) and the latter is in series with the inductor L. In this equivalent circuit, the polarization resistance ( $R_p$ ) can be calculated from equation 1[14, 15]:

$$R_p = (R_{ct} \times R_L) / (R_{ct} + R_L) \tag{1}$$

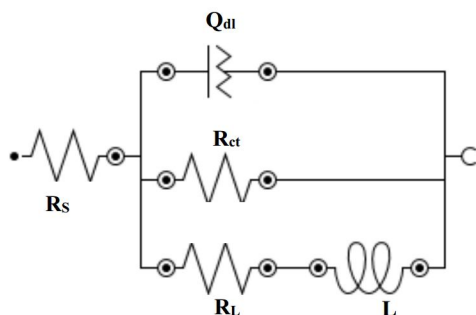


**Fig. 8.** The equivalent circuit used to model the Nyquist plots of both composites in 0.10 and 0.50M HCl solutions [13].

Table 4 presents the best fitting parameters obtained for the measured impedance data on both composites in 0.10 and 0.50 M HCl solutions.

It is seen that the measured value of polarization resistance decreases with increasing concentration of the acid, indicating that the corrosion rates of both composites increased with the increase in the concentration of HCl solutions. Also, it is clear that the polarization resistance of the composite cast by squeeze casting was higher than that of the composites cast by gravity. These results are in fully agreement with the results obtained from Tafel polarization data and the SEM micrographs of the surfaces of the gravity and squeeze casting composites.

#### 4. CONCLUSIONS

Based on the systematic study of the corrosion behaviour of A356-10 vol.% SiC composites cast by gravity and squeeze casting in different concentrations of HCl solutions by electrochemical methods the following conclusions are made:

1. The SEM micrographs of the A356-10 vol.% SiC composites showed that the squeeze casting exhibit a good dispersion/matrix interface when compared with the composite produced by gravity process.

2. In squeeze casting, a limited amount of interfacial porosity was observed in the composite when compared to that of gravity casting technique.
3. The Tafel polarization and EIS studies of the corrosion behaviour of the A356-10 vol.% SiC composites showed that the corrosion resistance of the composite cast by squeeze casting was higher than that of the composites cast by gravity in selected corrosion media.
4. Also, the Tafel polarization and EIS studies revealed that the corrosion current densities of both composites increase with the increase in the concentration of HCl.
5. EIS studies showed that as the concentration increases, the measured value of polarization resistance decreases for both composites. Also, EIS studies revealed that the polarization resistance of the composite cast by squeeze casting was higher than that of the composites cast by gravity in selected HCl solutions.

## REFERENCES

1. Daoud, A., and Reif, W., "Influence of Al<sub>2</sub>O<sub>3</sub> particulate on the aging response of A356 Al-based composites", *J. Mater. Process. Technol.*, 2002, 123, 313.
2. Vencl, A., Bobic, I., Arostegui, S., Bobic, B., Marinkovic, A., and Babic, M., "Structural, mechanical and tribological properties of A356 aluminium alloy reinforced with Al<sub>2</sub>O<sub>3</sub>, SiC and SiC + graphite particles", *J. Alloys Compd.*, 2010, 506, 631.
3. Ribes, H., and Suery, M., "Effect of particle oxidation on age hardening of Al-Si-Mg/SiC composites", *Scripta Metallurgica*, 1989, 23, 705.
4. Cholewa, M., "Simulation of solidification process for composite micro-region with incomplete wetting of reinforcing particle", *J. Mater. Process. Technol.*, 2005, 164, 1181.
5. Tjong, S. C., Wang, G. S., and Mai, Y. W., "High cycle fatigue response of in-situ Al-based composites containing TiB<sub>2</sub> and Al<sub>2</sub>O<sub>3</sub> submicron particles", *Compos. Sci. Technol.*, 2005, 65, 1537.
6. Li, G. R., Zhao, Y. T., Wang, H. M., Chen, G., Dai, Q. X., and Cheng, X. N., "Fabrication and properties of in situ (Al<sub>3</sub>Zr+Al<sub>2</sub>O<sub>3</sub>)p/A356 composites cast by permanent mould and squeeze casting", *J. Alloys Compd.*, 2009, 471, 530.
7. Zhiqiang, S., Di, Z., and Li, G., "Evaluation of dry sliding wear behavior of silicon particles reinforced aluminum matrix composites", *Mater. Des.*, 2005, 26, 454.
8. Kok, M., "Abrasive wear of Al<sub>2</sub>O<sub>3</sub> particle reinforced 2024 aluminium alloy composites fabricated by vortex method, *Composites A*", 2006, 37, 457.
9. Trowsdale, A. J., Noble, B., Harris, S. J., Gibbins, I. S. R., Thompson, G. E., and Wood, G. C., "The influence of silicon carbide reinforcement on the pitting behaviour of aluminium", *Corros. Sci.*, 1996, 38, 177.
10. Oguzie, E. E., "Corrosion inhibition of aluminium in acidic and alkaline media by *Sansevieria trifasciata* extract", *Corros. Sci.*, 2007, 49, 1527.
11. Mercier, D., Herinx, M., and Barthés-Labrousse, M. G., "Influence of 1, 2-diaminoethane on the mechanism of aluminium corrosion in sulphuric acid solutions", *Corros. Sci.*, 2010, 52, 3405.
12. Pinto, G. M., Nayak, J., and Shetty, A. N., "Corrosion Behaviour of 6061 Al - 15vol. Pct. SiC Composite and its Base Alloy in a Mixture of 1:1 Hydrochloric and Sulphuric Acid Medium", *Int. J. Electrochem. Sci.*, 2009, 4, 1452.
13. Lee, K. K., and Kim, K. B., "Electrochemical impedance characteristics of pure Al and Al-Sn alloys in NaOH solution", *Corros. Sci.*, 2001, 43, 561.
14. Pinto G. M., Nayak J., Shetty A. N., "Corrosion inhibition of 6061 Al-15 vol. pct. SiC(p) composite and its base alloy in a mixture of sulphuric acid and hydrochloric acid by 4-(N,N-dimethyl amino) benzaldehyde thiosemicarbazone", *Mater. Chem. Phys.*, 2011, 125, 628.
15. Bessone, J., Mayer, C., Juttner, and Lorenz, W. J., "AC-impedance measurements on aluminium barrier type oxide films", *Electrochim. Acta*, 1983, 28, 171.